BIOCELL
2020 44(1): 101-110

Tech Science Press

MicroRNA-145-3p suppresses the malignant behaviors of T-cell acute lymphoblastic leukemia Jurkat cells via inhibiting the NF-kappaB signaling pathway

Xin YANG*; Liqun LU; Li HUANG; Jing HE; Jie LV

Department of Pediatrics, The First Affiliated Hospital of Chengdu Medical College, Chengdu, China

Key words: T-cell acute lymphoblastic leukemia, Proliferation, Invasion, Resistance to apoptosis

Abstract: T-cell acute lymphoblastic leukemia (T-ALL) is a hematological tumor caused by the malignant transformation of immature T-cell progenitor cells. Emerging studies have stated that microRNAs (miRNAs) may play key roles in T-ALL progression. This study aimed to investigate the roles of miR-145-3p in T-ALL cell proliferation, invasion, and apoptosis with the involvement of the nuclear factor-kappaB (NF-κB) signaling pathway. T-ALL Jurkat cells were harvested, and the expression of miR-145-3p and NF-κB-p65 was measured. Gain- and loss-of-functions of miR-145-3p and NF-κB-p65 were performed to identify their roles in the biological behaviors of Jurkat cells, including proliferation, apoptosis, and invasion. Consequently, the current study demonstrated that miR-145-3p was down-regulated while NF-κB-p65 was up-regulated in Jurkat cells. miR-145-3p directly bound to the 3' untranslated region of NF-κB-p65. Over-expression of miR-145-3p inhibited Jurkat cell proliferation, invasion, and resistance to apoptosis, while over-expression of NF-κB-p65 presented opposite trends. Co-transfection of miR-145-3p and NF-κB-p65 promoted the malignant behaviors of Jurkat cells compared to miR-145-3p transfection alone, while it reduced these behaviors of Jurkat cells compared to NF-κB-p65 transfection alone. Taken together, this study provided evidence that miR-145-3p could suppress proliferation, invasion, and resistance to the death of T-ALL cells via inactivating the NF-κB signaling pathway.

Introduction

T-cell acute lymphoblastic leukemia (T-ALL) is a fast-growing blood malignancy that is caused by the clonal expansion of transformed T-cell precursors (Evangelisti *et al*., 2018). It accounts for approximately 12-15% of T-ALL cases in children and 25% in adults with unique clinical and biological features (Raetz and Teachey, 2016; Habiel *et al*., 2016). T-ALL is correlated with a variety of acquired genetic abnormalities that lead to developmental arrest and aberrant growth of malignant lymphoid progenitors (Bond *et al*., 2016). Most pediatric T-ALL patients are expected to be cured, and the survival rate of adults younger than 60 years subjected to conventional chemotherapy reached nearly 50%, while older patients have a more unfavorable prognosis (Gianfelici *et al*., 2016). Despite the advanced therapy protocols, there are still 15-25% of children and 40-50% adult T-ALL patients that relapse and develop drug resistance (Habiel *et al*., 2016). Moreover, the T-ALL survivors, particularly the children survivors, are at higher risk of acquiring long-run adverse health problems, such as secondary malignancies resulting from genotoxic drugs (Teepen *et al*., 2017). Therefore, novel and more effective therapeutic options are urgently needed to improve the outcome and life quality of T-ALL patients.

MicroRNAs (miRNAs) are a class of endogenous short non-coding RNAs that post-transcriptionally regulate protein-coding genes via binding to the 3' untranslated regions (3' UTR) of target mRNAs, contributing to mRNA degradation or translational inhibition (Shioya *et al*., 2010). miRNAs may play a crucial regulatory role in key cellular processes, including cell growth, cell cycle, or cell apoptosis (Coskun *et al*., 2011). One single miRNA can mediate thousands of mRNAs, and over 60% of human protein-coding genes are mediated by miRNAs (Lewis *et al*., 2005). Emerging studies suggest that miRNAs might play significant roles in the pathogenesis of human leukemia (Seca H *et al*., 2010; Qian Lu *et al*., 2016). Meanwhile, miR-145-3p has been suggested to act as a tumor suppressor in several cancer types (Goto *et al*., 2017; Chen *et al*., 2018). While the effect of miR-145-3p on T-ALL remains unknown. Importantly, our study identified that miR-145-3p directly bound to the 3'UTR of NF-κB-p65. The NF-κB pathway is a key regulator of apoptosis and plays significant roles in many normal cellular functions (Yu *et al*., 2017). Aberrant activation of the NF-κB pathway has been suggested to be involved in the

*Address correspondence to: Xin Yang,
Dr___YangXin@163.com

Doi: 10.32604/biocell.2020.08324

pathogenesis of several tumors (Wang *et al*., 2009; Kuck *et al*., 2017), as well as in ALL cells (Kordes *et al*., 2000). Taken together, the current study was designed to explore the role of miR-145-3p in the development of T-ALL with the involvement of the NF-κB signaling pathway.

Materials and Methods

Cell culture and grouping

Human T-acute lymphoblastic leukemia (T-ALL) Jurkat cell line purchased from American Type Culture Collection (Rockville, MD, USA) were cultured in Roswell Park Memorial Institute (RPMI) 1640 complete medium containing 10% fetal bovine serum (FBS), 100 μg/mL streptomycin and 100 U/mL penicillin in a 37°C incubator with 5% CO_2. The medium was refreshed 3-4 times each week until the cell confluence reached 80%, after which the cells began to be passaged. Mononuclear cells (MNCs) collected from human blood from five healthy volunteers (people with major diseases or infectious diseases were excluded). The study was approved by the Ethics committee of the First Affiliated Hospital of Chengdu Medical College, and signed informed consent was obtained from each eligible volunteer.

Jurkat cells in the logarithmic growth phase were seeded into 6-well plates at a density of 5×10^5 cells/mL. Next, the cells were assigned into control, mimic negative control (NC), miR-145-3p mimic, inhibitor NC, miR-145-3p inhibitor, over-expression (oe)-NF-κB-p65 and miR-145-3p mimic + oe-NF-κB-p65 groups after corresponding transfections. All transfections were performed following the instructions of the Lipofectamine™ 2000 kit (Invitrogen Inc., Carlsbad, CA, USA), with all the plasmids purchased from Shanghai GenePharma Co., Ltd. (Shanghai, China). Briefly, 5 μg plasmids and 10 μL Lipofectamine™ 2000 were diluted with 250 μL serum-free Opti-MEM (Gibco Company, Grand Island, NY, USA) and mixed, respectively. Followed by standing at room temperature for 5 min, the two tubes were mixed and allowed to stand for 20 min. Then the mixture was seeded into wells and incubated at 37°C with 5% CO_2 for 8 h, after which the medium was refreshed as complete medium for 72 h of culture, and the cells were collected for following experiments.

Dual luciferase reporter gene assay

A computer-based miR target detection program (http://www.targetscan.org) was performed to predict the binding sites of miR-145-3p and NF-κB-p65. The pMIR-based reporter plasmids (Beijing Huayueyang Biotechnology Inc, Beijing, China) containing wild-type NF-κB-p65 (pMIR-NF-κB-p65-WT) or NF-κB-p65 mutated at the putative miRNA-145-3p binding sites (pMIR-NF-κB-p65-MT) were designed. Well-designed pMIR-based reporter plasmids along with either miRNA-145-3p mimic or mimic NC were co-transfected into HEK293T cells (Shanghai Cell Bank of the Chinese Academy of Sciences, Shanghai, China), with pMIR-Renilla luciferase used as an internal reference. Cells were lysed 48 h after transfections. Relative luciferase activity was normalized to that of Renilla luciferase and determined using the dual-luciferase reporter assay system according to the kit's instructions (E1910, Promega Corp., Madison, Wisconsin, USA). The relative value of firefly luciferase activity/Renilla luciferase activity was evaluated and analyzed.

Reverse transcription-quantitative polymerase chain reaction (RT-qPCR)

Total RNA was extracted using Trizol reagent (Invitrogen, Carlsbad, CA, USA). The RNA concentration was measured using a Nanodrop 2000 spectrophotometer (Thermo Fisher Scientific Inc., Waltham, MA, USA), and 1 μg of RNA was reversely transcribed into cDNA using a PrimeScript™ RT reagent kit with gDNA Eraser (Takara Holdings Inc., Kyoto, Japan) following the kit's instructions. Briefly, extracted RNA was treated with 200 μL 5× gDNA Eraser Buffer and 100 μL gDNA Eraser at 42°C for 2 min for DNA exclusion. RT was performed at 37°C for 15 min and 85°C for 5 s to produce cDNA. Next, the real time-PCR was performed using a SYBR® Premix Ex Taq™ (TliRNase H Plus) assay kit (Takara Holdings Inc., Kyoto, Japan) on an ABI7500 qPCR kit (Thermo Fisher Scientific Inc., Waltham, MA, USA). The PCR conditions were as follow: predenaturation at 95°C for 10 min, followed by 40 cycles of denaturation at 95°C for 15 s, annealing at 60°C for 30 s, and a final extension at 72°C for 30 s. U6 was set as an internal control for miR-145-3p expression while glyceraldehyde-3-phosphate dehydrogenase (GAPDH) was set as an internal control for other genes. The $2^{-\Delta\Delta Ct}$ method was applied in which $2^{-\Delta\Delta Ct}$ refers to the ratio of the target gene expression between experimental group and control group, the formula was as follows: $\Delta\Delta Ct = [Ct \text{ (target gene)-Ct (internal control gene)}]_{\text{experimental group}} - [Ct \text{ (target gene)-Ct (internal control gene)}]_{\text{control group}}$. The Ct value was determined by the PCR cycle number at which fluorescence reaches a threshold value, during which the amplification was in logarithmic growth. The primers (Tab. (1)) were provided by Shanghai GenePharma Co., Ltd. (Shanghai, China).

TABLE 1

Primer sequences for RT-qPCR

Gene	Primer sequence (5'-3')
miR-145-3p	F: GGGGATTCCTGGAAATA
	R: TGCGTGTCGTGGAGTC
U6	F: GCTTCGGCAGCACATATACTAAAAT
	R: CGCTTCACGAATTTGCGTGTCAT
NF-κB-p65	F: CTGAACCAGGGCATACCTGT
	R: GAGAAGTCCATGTCCGCAAT
Bcl-2	F: CGACGACTTCTCCCGCCGCTACCGC
	R: CCGCATGCTGGGGCCGTACAGTTCC
Bax	F: TCCACCAAGAAGCTGAGCGAG
	R: GTCCAGCCCATGATGGTTCT
MMP-9	F: TCCCTGGAGACCTGAGAACC
	R: CGGCAAGTCTTCCGAGTAGTTT
E-cadherin	F: ACCTCCGTGATGGAGGTC
	R: CCACATTCGTCACTGCTACG
GADPH	F: TCCTCTGACTTCAACAGCGACACC
	R: TCTCTCTTCCTCTTGTGCTCTTGG

Note: miR, microRNA; NF-κB, nuclear factor-kappa B, MMP-9, matrix metalloproteinase-9; GAPDH, Glyceraldehyde-3-phosphate dehydrogenase; F, forward; R, reverse.

Western blot analysis

Total proteins of cells were extracted, and then the protein concentration was detected using a bicinchoninic acid (BCA) kit (Thermo Fisher Scientific Inc., Waltham, MA, USA). Extracted proteins were separated by 10% sodium dodecyl sulfate-polyacrylamide gel electrophoresis (SDS-PAGE) and transferred onto polyvinylidene difluoride (PVDF) membranes (Merck Millipore Co., Billerica, MA, USA) with the voltage from 80 V (35 min) to 120 V (45 min). Followed by 5% bovine serum albumin (BSA) sealing for 1 h at room temperature and PBST (phosphate buffer saline (PBS) + 0.1% Tween 20) washing, the membranes were incubated with the following primary antibodies at 4°C overnight: NF-κB-p65 rabbit monoclonal antibody (1: 5000, ab51248, Abcam Inc., Cambridge, MA, USA), Bcl-2 (1:1000, 4223, Cell Signaling Technology (CST), Beverly, MA, USA) and Bax rabbit polyclonal antibody (1:1000, 2774, Abcam). Next, the membranes were washed with PBST three times, 10 min each. Thereafter, the membranes were incubated with horseradish peroxidase-labeled goat anti-rabbit and goat anti-mouse secondary antibodies (1:10000, Jackson, USA) at room temperature for 1 h, after which they were washed with PBST buffer three times, 10 min each. Then the membranes were soaked into an enhanced chemiluminescence (ECL) system (Pierce, Waltham, MA, USA) at room temperature for 1 min. Then the liquid was discarded, and the membranes were covered with plastic wraps, exposed, visualized, and fixed in the dark, after which the bands were analyzed using ImageJ software (National Institutes of Health, Bethesda, Maryland, USA). One-way analysis of variance (ANOVA) was applied for data analysis, and each experiment was repeated three times.

3-(4,5-dimethylthiazol-2-yl)-2,5-diphenyltetrazolium bromide (MTT) assay

When the cell confluence reached 80-90%, the Jurkat cells in each group were seeded into 96-well plates. Next, the media were discarded at 24, 48, 72, and 96 h, respectively, and replaced as 100 μL medium containing 10% MTT solution (Cat. No. M1020, Beijing Solarbio Science & Technology Co., Ltd., Beijing, China). Followed by 4 h of incubation, the supernatant was discarded carefully, and then the sediments were dissolved with 110 μL formazan. Then the optical density (OD) value at 490 nm was detected using a microplate reader (DNM-9602G; Aolu Biotech, Shanghai, China).

Flow cytometry

Cell apoptosis was detected using flow cytometry. In brief, 48 h after transfection, cells were detached with trypsin, and then the cell suspension was collected, centrifuged, washed twice with PBS and centrifuged again. Then the cells were collected for further experiments. Cell apoptosis was detected as follows: cells were resuspended with PBS, and the resuspension (about 1×10^4 cells) was centrifuged with the supernatant discarded. After that, the cells were gently resuspended with 195 μL binding buffer, and then added with 5 μL annexin V-fluorescein isothiocyanate (FITC) and 10 μL propidium iodide (PI). The mixture was then allowed to stand at room temperature in the dark for 20 min, ice bathed, and then detected on a flow cytometer (C1063, Beyotime Biotechnology Co., Ltd., Shanghai, China). The experiment was repeated three times. Cell cycle measurement: cells were fixed with 1 mL pre-cooled 75% ethanol (-20°C) at 4°C overnight. Thereafter, the cells were washed with cold PBS twice. The PI staining solution was prepared, and each sample was stained with 535 μL mixture containing 500 μL binding buffer, 25 μL PI staining solution (20×), and 10 μL RNase (50×). Cells were treated with 500 μL PI binding buffer, resuspended, bathed at 37°C in the dark for 30 min, and detected using a flow cytometer (C1052, Beyotime Biotechnology Co., Ltd., Shanghai, China) at 4°C in the dark. The experiment was repeated three times.

Transwell assay

Forty-eight hours after transfection, cells were successively cultured in serum-free medium, starved for 24 h, trypsinized, washed twice with PBS, and then resuspended with serum-free medium for following experiments. The 24-well (8 μm) transwell plates (Corning Glass Works, Corning, NY, USA) were used in this study, with three wells set for each group. The wells were firstly coated with 50 μL serum-free-medium diluted Matrigel (1:5, Sigma-Aldrich Chemical Company, St Louis, MO, USA). Followed by 4-5 h of air drying at 37°C, the apical chamber was added with serum-free RPMI 1640 medium to produce 200 μL cell suspension with the cell density adjusted to 1×10^5 cells/mL, while the basolateral chamber was added with 500 μL RPMI 1640 complete medium containing 10% FBS. Twenty-four hours later, the transwells were taken out, washed twice with PBS, and fixed with 5% glutaraldehyde for 30 min, which was followed by gentian violet staining for 5 min. Then the number of stained cells was calculated under an inverted microscope (Olympus Optical Co., Ltd., Tokyo, Japan). The number of invaded cells was observed under a fluorescence microscope with five views randomly selected. Three duplicated wells were set for each group, and the experiments were performed three times with the average value calculated.

Statistical analysis

The Statistical Package for the Social Sciences (SPSS) 21.0 (IBM Co. Armonk, NY, USA) was applied for data analysis. Measurement data were expressed as mean ± standard deviation. Differences between every group pair were analyzed using the t-test, while among multiple groups were compared using one-way analysis of variance (ANOVA) and Bonferroni correction was applied for pair comparisons after ANOVA. $p < 0.05$ (two-tailed test) was considered to show a statistically significant difference.

Results

The relative expression of miR-145-3p is lower in Jurkat cells opposite to NF-κB-expression in comparison to MNCs

RT-qPCR was applied to measure the miR-145-3p and NF-κB-p65 expression in MNCs and Jurkat cells, which suggested that miR-145-3p expression was relatively lower while NF-κB-p65 expression was relatively higher in Jurkat cells than in MNCs (Figs. 1(A)-1(B)) (all $p < 0.05$). Correspondingly, the Western blot analysis results presented the same trends (Fig.

1(C)) ($p < 0.05$).

miR-145-3p negatively targets NF-κB-p65

The computer-based program (http://www.targetscan.org) prediction suggested that miR-145-3p could directly bind to the 3'UTR of NF-κB-p65 (Fig. 2(A)). Correspondingly, cells co-transfected with miR-145-3p and NF-κB-WT presented a significantly decreased luciferase activity compared to those transfected with NF-κB-MT according to the dual-luciferase reporter gene assay (Fig. 2(B)). To further identify the correlation between miR-145-3p and NF-κB-p65, Jurkat cells were transfected with either miR-145-3p mimic or miR-145-3p inhibitor, after which the miR-145-3p expression in cells was correspondingly elevated or decreased compared to the control or the cells transfected with mimic NC as RT-qPCR identified (all $p < 0.05$) (Fig. 2(C)). Thereafter, Western blot analysis was applied to measure NF-κB-p65 protein expression, which demonstrated that over-expression of miR-145-3p decreased NF-κB-p65 protein expression in Jurkat cells, while down-regulated miR-145-3p presented an opposite tread (all $p < 0.05$).

Up-regulated miR-145-3p inhibits Jurkat cell proliferation and growth

The MTT assay results suggested that over-expression of miR-145-3p significantly reduced the Jurkat cell proliferation 96 h after transfection, while over-expression of NF-κB-p65 notably elevated cell proliferation. Co-transfection with miR-145-3p mimic and oe-NF-κB-p65 led to significantly enhanced cell proliferation compared to miR-145-3p mimic transfection alone, and correspondingly, this co-transfection led to an obvious, reduced cell proliferation compared to oe-NF-κB-p65 transfection alone (all $p < 0.05$) (Fig. 3). These results suggested that up-regulated NF-κB-p65 could promote Jurkat cell proliferation, while overexpression of miR-145-3p could suppress this promotion.

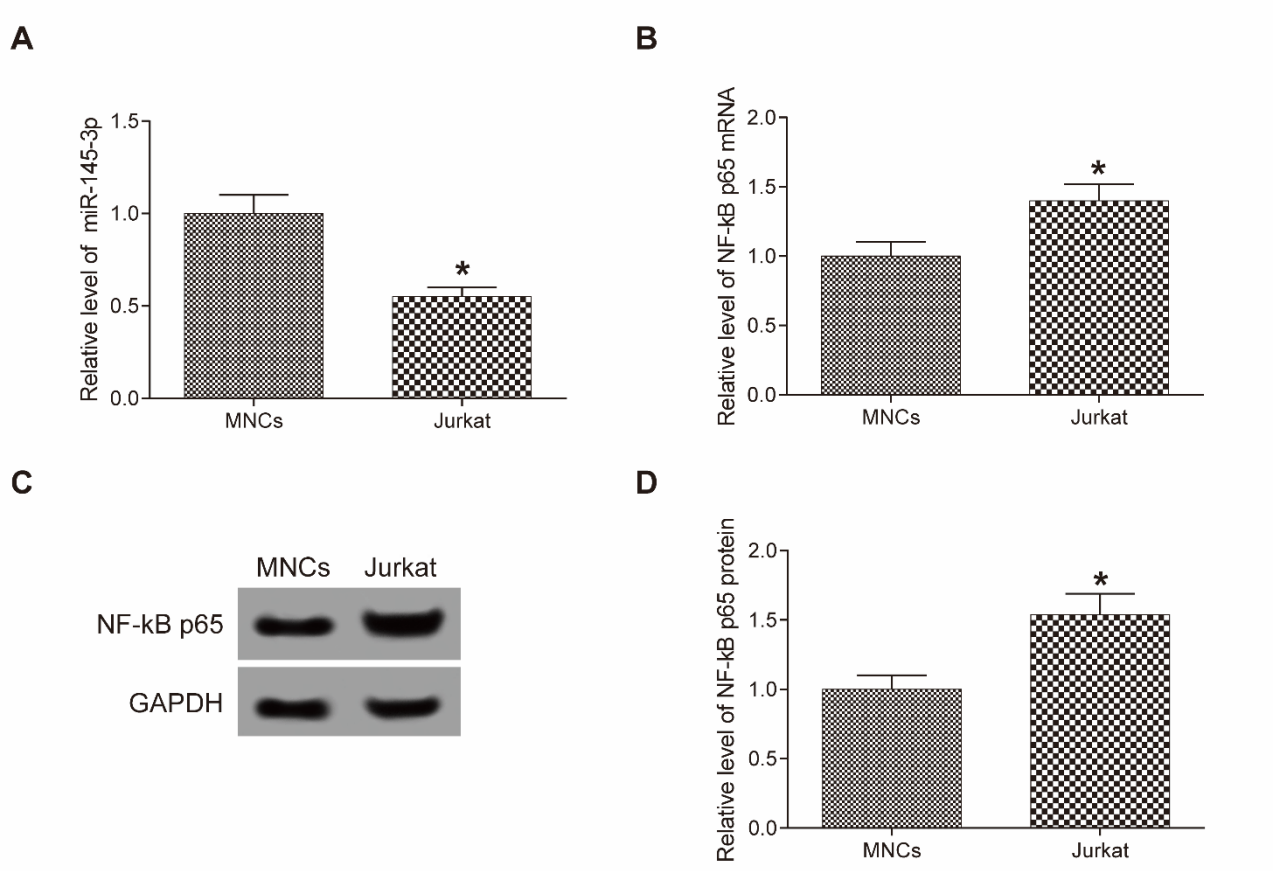

FIGURE 1. miR-145-3p is up-regulated while NF-κB-p65 is down-regulated in Jurkat cells. Note: A-B, expression of miR-145-3p (A) and mRNA expression of NF-κB-p65 (B) in Jurkat cells measured using RT-qPCR; C, protein expression of NF -κB detected using Western blot analysis. Repetition = 3; data were analyzed using the *t* test and expressed as mean ± standard deviation. *, compared to the MNCs, $p < 0.05$; miR-145-3p, microRNA-145-3p, NF-κB, nuclear factor-kappa B; RT-qPCR, reverse transcription-quantitative polymerase chain reaction; MNCs, mononuclear cells.

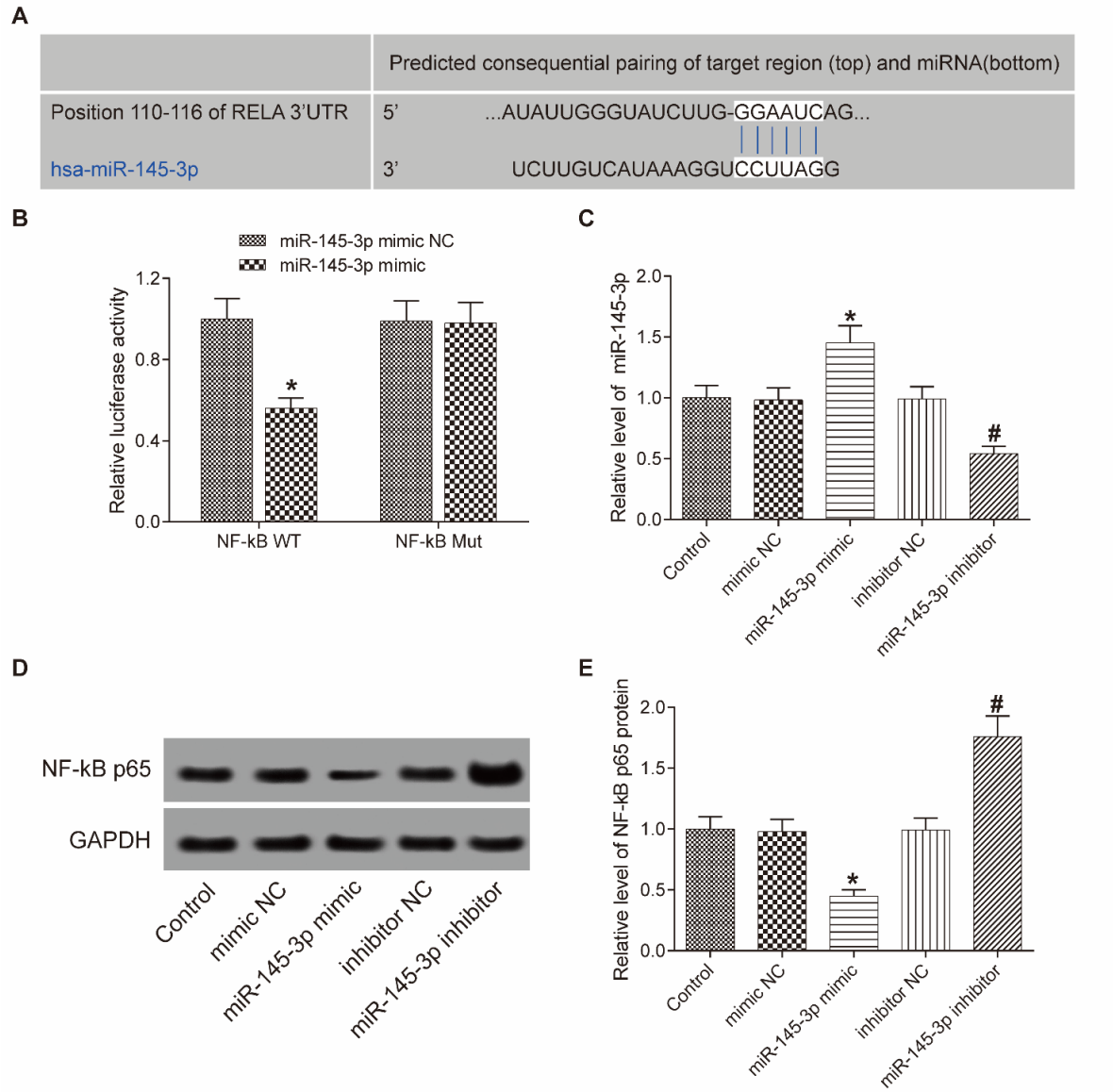

FIGURE 2. miR-145-3p negatively targets NF-κB-p65. Note: A, prediction of the binding of miR-145-3p and NF-κB-p65 performed via an online website (http://www.targetscan.org); B, binding relation of miR-145-3p and NF-κB-p65 identified using dual luciferase reporter gene assay; C, miR-145-3p expression measured using RT-qPCR; D, NF-κB-p65 expression detected using Western blot analysis. Repetition = 3, data were analyzed using one-way ANOVA and expressed as mean ± standard deviation; *, compared to the mimic NC group, $p < 0.05$; # compared to the inhibitor NC group, $p < 0.05$; miR-145-3p, microRNA-145-3p, NF-κB, nuclear factor-kappa B; RT-qPCR, reverse transcription-quantitative polymerase chain reaction; ANOVA, analysis of variance; NC, negative control.

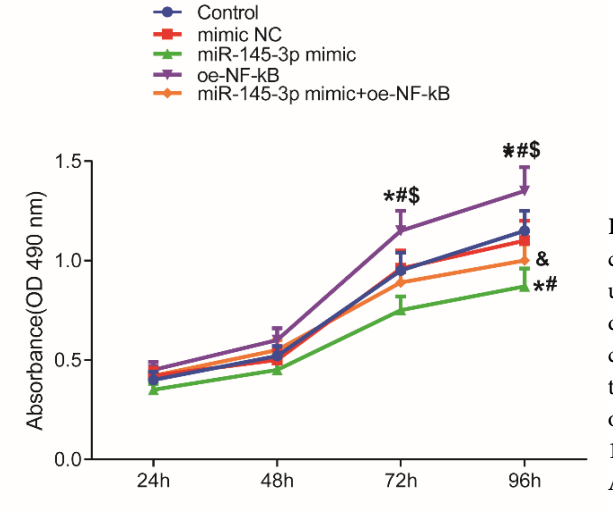

FIGURE 3. Over-expressed miR-145-3p inhibits Jurkat cell proliferation. Note: Repetition = 3, data were analyzed using one-way ANOVA and expressed as mean ± standard deviation; *, compared to the control group, $p < 0.05$; #, compared to the mimic NC group, $p < 0.05$; $ compared to the miR-145-3p mimic group, $p < 0.05$; & compared to the oe-NF-κB-p65 group, $p < 0.05$; miR-145-3p, microRNA-145-3p, NF-κB, nuclear factor-kappa B; oe, over-expression; ANOVA, analysis of variance; NC, negative control.

Up-regulated miR-145-3p induces cell cycle arrest and apoptosis of Jurkat cells

Cell apoptosis and cell cycle were measured using flow cytometry. The apoptosis detection suggested that cells in the control group and mimic group presented no obvious difference. While up-regulated miR-145-3p markedly enhanced cell apoptosis, but over-expressed NF-κB-p65 presented an opposite trend (all $p < 0.05$). Meanwhile, the co-transfection of miR-145-3p mimic and oe-NF-κB-p65 led to reduced apoptosis compared to miR-145-3p transfection alone, while it led to enhanced cell apoptosis compared to oe-NF-κB-p65 transfection alone (all $p < 0.05$) (Fig. 4(A)). Likewise, cells in the control group and mimic group presented no obvious difference in terms of the cell cycle. But the proportion of Jurkat cells in the G_0/G_1 phase in those with over-expression of miR-145-3p was notably increased compared to the control, while cells with over-expression of NF-κB-p65 presented an opposite trend. Moreover, the co-transfection of miR-145-3p mimic and oe-NF-κB-p65 led to reduced G_0/G_1 proportion of cells compared to miR-145-3p mimic transfection alone while increased the G_0/G_1 proportion in cells transfected with oe-NF-κB-p65 alone (all $p < 0.05$) (Fig. 4(B)). These results identified that over-expressed miR-145-3p or down-regulated NF-κB-p65 could induce cell cycle arrest and apoptosis of Jurkat cells.

Up-regulated miR-145-3p enhances the Bax/Bcl-2 ratio in Jurkat cells

RT-qPCR and Western blot analysis were applied to measure the Bax and Bcl-2 expression in Jurkat cells, which suggested that overexpression of miR-145-3p enhanced Bax while reduced Bcl-2 expression, and overexpression of NF-κB-p65 led to an opposite trend ($p < 0.05$) (Figs. 5(A)-5(B)). Meanwhile, the combined use of miR-145-3p mimic and oe-NF-κB-p65 reduced Bax while elevated Bcl-2 expression compared to use of miR-145-3p mimic alone, while it resulted in converse trends compared to the use of oe-NF-κB-p65 alone (all $p < 0.05$) (Figs. 5(A)-5(B)).

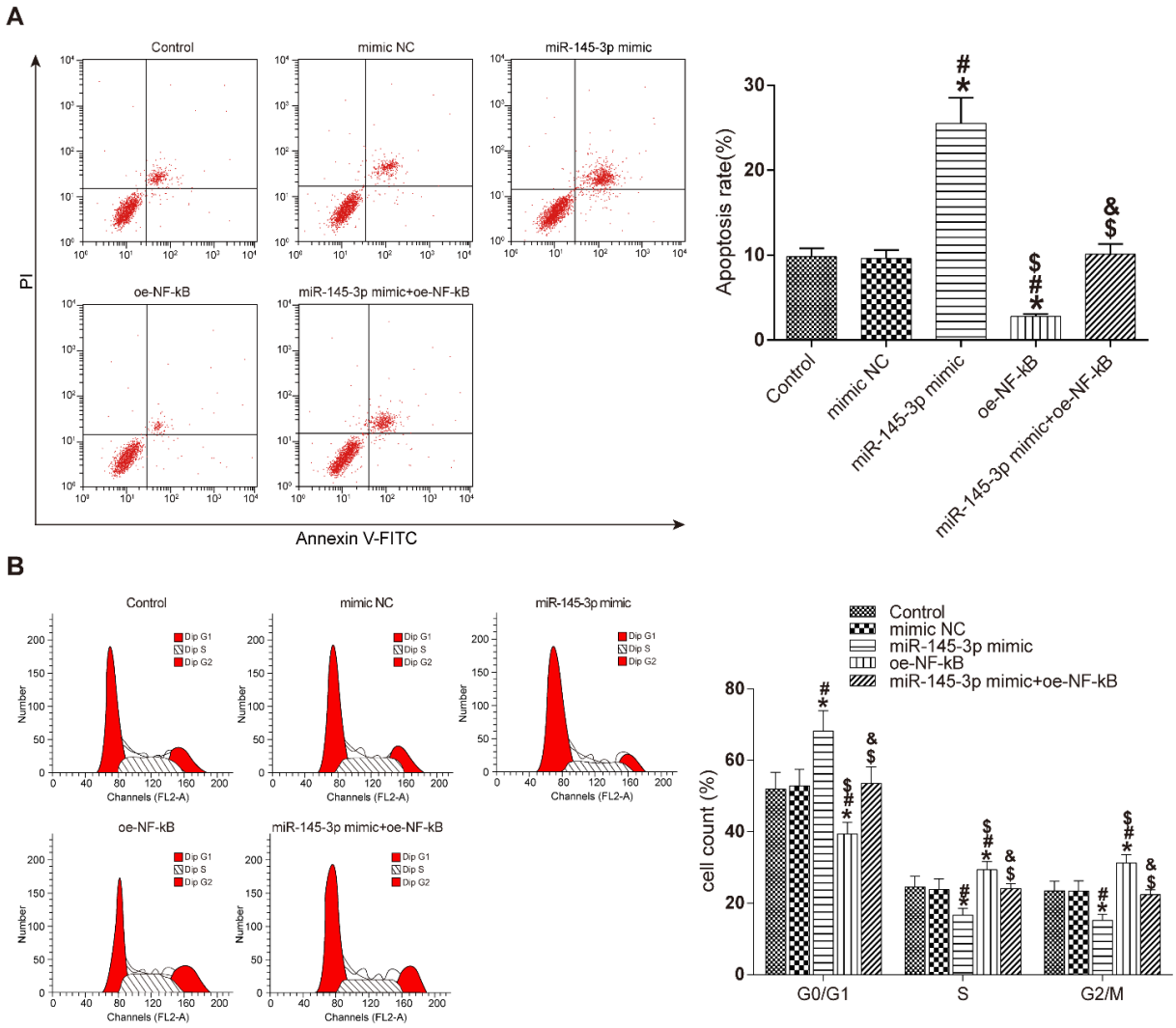

FIGURE 4. Over-expressed miR-145-3p/down-regulated NF-κB-p65 induces cell cycle arrest and apoptosis of Jurkat cells. Note: A, Jurkat cell apoptosis measured via flow cytometry; B, cell cycle of Jurkat cells measured using flow cytometry. Repetition = 3, data were analyzed using one-way ANOVA and expressed as mean ± standard deviation; *, compared to the control group, $p < 0.05$; #, compared to the mimic NC group, $p < 0.05$; $ compared to the miR-145-3p mimic group, $p < 0.05$; & compared to the oe-NF-κB-p65 group, $p < 0.05$; miR-145-3p, microRNA-145-3p, NF-κB, nuclear factor-kappa B; oe, over-expression; ANOVA, analysis of variance; NC, negative control.

Up-regulated miR-145-3p inhibits Jurkat cell invasion

The transwell result suggested that up-regulated miR-145-3p significantly reduced cell invasion, but over-expression of NF-κB-65 enhanced that (all $p < 0.05$). Meanwhile, the co-effect of miR-145-3p and NF-κB-65 presented increased invasion compared to over-expression of miR-145-3p alone while showed decreased invasion compared to over-expression of NF-κB-65 alone (all $p < 0.05$) (Fig. 6(A)).

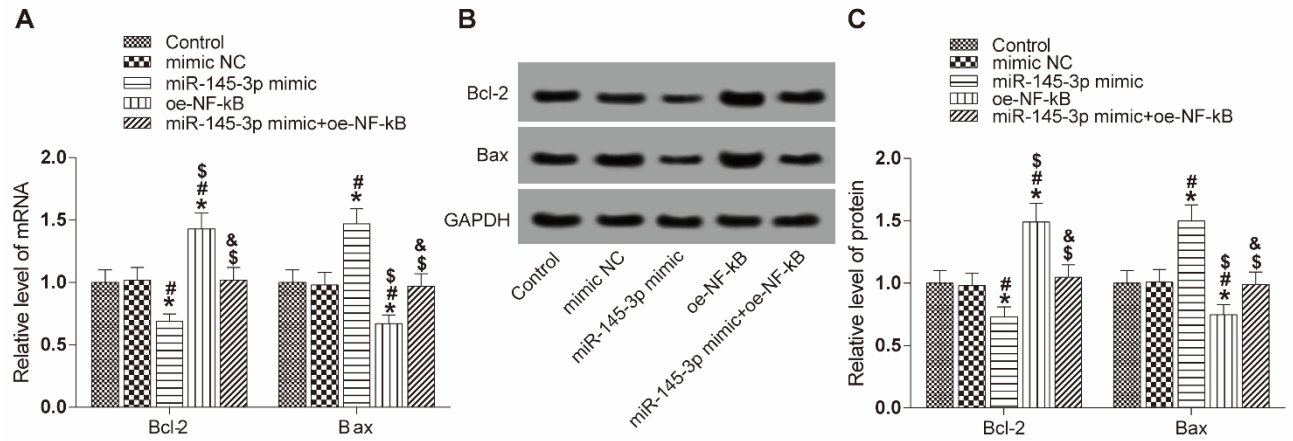

FIGURE 5. Over-expressed miR-145-3p enhances the Bax/Bcl-2 ratio in Jurkat cells. Note: A-B, mRNA expression (A) and protein levels (B) of Bax and Bcl-2 in Jurkat cells measured using RT-qPCR and Western blot analysis, respectively. Repetition = 3, data were analyzed using one-way ANOVA and expressed as mean ± standard deviation; * compared to the control group, $p < 0.05$; $^{\$}$ compared to the miR-145-3p mimic group, $p < 0.05$; $^{\&}$ compared to the oe-NF-κB-p65 group, $p < 0.05$; miR-145-3p, microRNA-145-3p, NF-κB, nuclear factor-kappa B; RT-qPCR, reverse transcription-quantitative polymerase chain reaction; oe, over-expression; ANOVA, analysis of variance; NC, negative control.

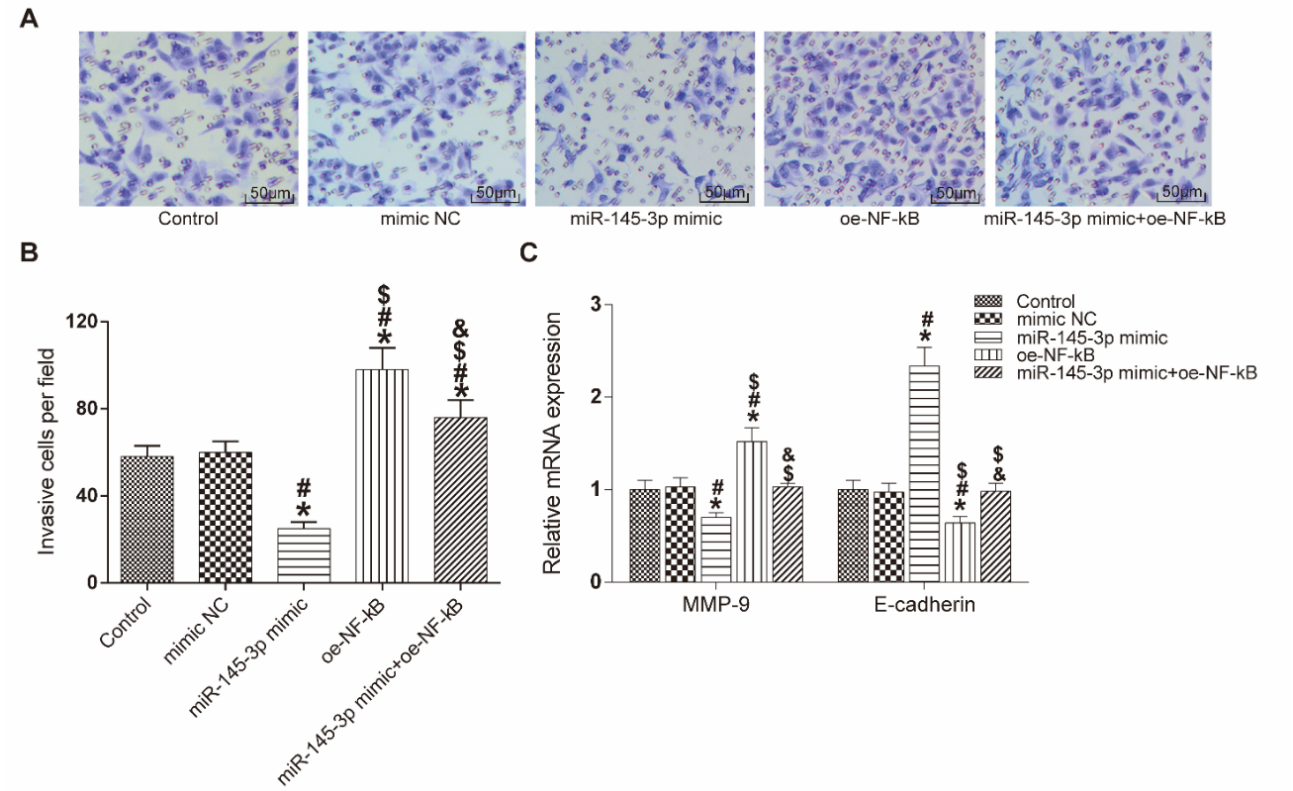

FIGURE 6. Up-regulated miR-145-3p inhibits Jurkat cell invasion. Note: A, cell invasion detected with Transwell assay and observed under a microscope (bar = 50 μm); B, mRNA expression of invasion-related factors MMP-9 and E-cadherin using RT-qPCR. Repetition = 3, data were analyzed using one-way ANOVA and expressed as mean ± standard deviation; * compard to the control group, $p < 0.05$; $^{\$}$ compared to the miR-145-3p mimic group, $p < 0.05$; $^{\#}$ compared to the mimic NC group, $p < 0.05$; $^{\&}$ compared to the oe-NF-κB-p65 group, $p < 0.05$; miR-145-3p, microRNA-145-3p, NF-κB, nuclear factor-kappa B; MMP-9, matrix metalloproteinase-9; RT-qPCR, reverse transcription-quantitative polymerase chain reaction; oe, over-expression; ANOVA, analysis of variance; NC, negative control.

The expression of invasion-related factors MMP-9 and E-cadherin were measured using RT-qPCR, which suggested that up-regulated miR-145-3p reduced MMP-9 expression while enhanced E-cadherin expression in Jurkat cells, while up-regulated NF-κB-65 led to converse outcomes (all $p < 0.05$) (Fig. 6(A)). Likewise, the combined use of miR-145-3p and NF-κB-65 led to enhanced MMP-9 expression but decreased E-cadherin expression compared to over-expression of miR-145-3p alone, while it led to declined MMP-9 expression but elevated E-cadherin expression compared to over-expression of NF-κB-65 alone (all $p < 0.05$) (Fig. 6(B)).

Discussion

Leukemia is a result of aberrant regulation of myeloid or lymphoid commitment during hematopoiesis (Lv *et al*., 2012). While differential miRNA expression found during hematopoiesis suggests that abnormal expression of miRNAs may be correlated with leukemogenesis (Yendamuri and Calin GA, 2009; Garzon and Croce, 2008), this study was carried out to investigate the role of miR-145-3p in T-ALL development and found that over-expression of miR-145-3p could inhibit the growth and malignant behaviors of T-ALL cells.

The initial finding of the current study was that miR-145-3p expression was relatively higher, while NF-κB-p65 was relatively lower in T-ALL Jurkat cells than in human MNCs. It has been suggested that miR-145 expression was significantly inhibited in ALL cells (Batliner *et al*., 2012). Moreover, we found that NF-κB-p65 is a target gene of miRNA-145-3p according to the evidence of online software analysis and dual-luciferase gene reporter assay, which was in coincidence with a previous study (Wen *et al*., 2014). Meanwhile, a recent study mentioned that human T-cell leukemia virus proteins may regulate NF-κB activation (Fochi *et al*., 2019). Also, NF-κB-p65 has been revealed to be up-regulated in nucleated peripheral blood cells from leukemia patients (Zhang *et al*., 2015).

Following the results above, the focus of the experiment shifted to figuring out the roles of miR-145-3p and NF-κB-p65 in Jurkat cell growth. Our study identified that overexpression of miR-145-3p inhibited Jurkat cell proliferation and invasion and resistance to apoptosis. A former study identified that miR-145 specifically could suppress tumor cell growth, and its down-regulation could lead to worse prognosis and a lower overall survival rate for T-ALL patients (Xia *et al*., 2014). Meanwhile, miR-145 has also been demonstrated to act as a tumor suppressor in other cancers. For instance, miR-145 could inhibit drug-resistant prostate cancer pathogenesis (Kato M *et al*., 2017). Similarly, miR-145 has been demonstrated to suppress bladder cancer growth via specific signaling pathways (Yoshino H *et al*., 2013). miR-145-3p is the passenger strand of miR-145 and is down-regulated in several types of cancer types as well as the guide strand miR-145-5p (Misono *et al*., 2019). Similarly, down-regulation of miR-145-3p has been observed in tissues and cells of several types of metastatic cancers such as breast, prostate, and lung cancers (Kumoğlu *et al*., 2019). On the other hand, NF-κB-p65 activation could rescue the leukemia cells from apoptosis (Nugues *et al*., 2014). Inhibition of NF-κB has also been suggested to markedly enhance apoptosis of leukemia cells (Dai *et al*., 2005). Besides, overexpression of miR-145-3p and the corresponding NF-κB-p65 significantly enhanced Bax expression while reduced Bcl-2 expression in Jurkat cells. miR-145 has been shown to up-regulate the Bax/Bcl2 ratio in non-small cell lung cancer cells (Pan *et al*., 2018). Bax are well-recognized apoptosis-related factors whose high expression could lead to apoptosis (Szobi *et al*., 2014; Fan *et al*., 2016). Bcl-2 is an anti-apoptotic protein that modulates the permeability of the mitochondrial membrane, while Bax could damage the outer mitochondrial membrane, thus promoting cell apoptosis (Lv *et al*., 2018). Moreover, our study found that the up-regulation of miR-145-3p led to decreased MMP-9 expression but elevated E-cadherin expression. MMP-9, a member of the MMP family, is well-known for the promoting effect on cell invasion (Ogasawara Nobutaka *et al*., 2018). E-cadherin is a junction protein between cells and always depleted during the epithelial-to-mesenchymal transition and further cell invasion (Zhao *et al*., 2014). Hence, it can be concluded that overexpression of miR-145-3p is capable of inhibiting proliferation and invasion and promoting apoptosis of T-ALL Jurkat cells.

As a minor strand of miR-145, the roles of miR-145-3p in diseases are less studied, and the roles of miR-145-3p in T-ALL have never been elucidated before. Here, our study identified that miR-145-3p may suppress the proliferation, invasion, and resistance to apoptosis growth of T-ALL Jurkat cells, possibly through inactivating the NF-κB signaling pathway. We hope these findings could provide new insights into the pathogenesis of T-ALL and the development of novel therapeutic options for T-ALL treatment.

Acknowledgement

Not applicable.

Conflicts of Interest

We declare no conflicts of interest.

References

Batliner J, Buehrer E, Fey MF, Tschan MP (2012). Inhibition of the miR-143/145 cluster attenuated neutrophil differentiation of APL cells. *Leukemia Research* **36**: 237-240.

Bond J, Marchand T, Touzart A, Cieslak A, Trinquand A, Sutton L, Radford-Weiss, Ludovic Lhermitte I, Spicuglia S, Dombret H, Macintyre E, Ifrah N, Hamel JF, Asnafi V (2016). An early thymic precursor phenotype predicts outcome exclusively in HOXA-overexpressing adult T-cell acute lymphoblastic leukemia: a group for research in adult acute lymphoblastic leukemia study. *Haematologica* **101**: 732-740.

Chen GM, Zheng AJ, Cai J, Han P, Ji HB, Wang LL (2018). microRNA-145-3p inhibits non-small cell lung cancer cell migration and invasion by targeting PDK1 via the mTOR signaling pathway. *Journal of Cellular Biochemistry* **119**: 885-895.

Coskun E, Heide EK, Schlee C, Kühnl A, Gökbuget N, Hoelzer D, Hofmann WK, Thiel E, Baldus CD (2011). The role of microRNA-196a and microRNA-196b as ERG regulators in acute myeloid leukemia and acute T-lymphoblastic leukemia. *Leukemia Research* **35**: 208-213.

Dai Y, Rahmani M, Dent P, Gant S (2005). Blockade of histone deacetylase inhibitor-induced RelA/p65 acetylation and NF-kappaB activation potentiates apoptosis in leukemia cells through a process mediated by oxidative damage, XIAP downregulation, and c-Jun N-terminal kinase 1 activation. *Molecular and Cellular Biology* **25**: 5429-5444.

Evangelisti C, Chiarini F, McCubrey JA, Martelli AM (2018). Therapeutic targeting of mTOR in T-cell acute lymphoblastic leukemia: an update. *International Journal of Molecular Sciences* **19**: 1878.

Fan Y, Lu H, An L, Wang C, Zhou Z, Feng F, Ma H, Xu Y, Zhao Q (2016). Effect of active fraction of *Eriocaulon sieboldianum* on human leukemia K562 cells via proliferation inhibition, cell cycle arrest and apoptosis induction. *Environmental Toxicology and Pharmacology* **43**: 13-20.

Fochi S, Bergamo E, Serena M, Mutascio S, Journo C, Mahieux R, Ciminale V, Bertazzoni U, Zipeto D, Romanelli MG (2019). TRAF3 is required for NF-κB pathway activation mediated by HTLV Tax proteins. *Frontiers in Microbiology* **10**: 1302.

Garzon R, Croce CM (2008). MicroRNAs in normal and malignant hematopoiesis. *Current Opinion in Hematology* **15**: 352-358.

Gianfelici V, Chiaretti S, Demeyer S, Giacomo FD, Messina M, Starza RL, Peragine N, Paoloni F, Geerdens E, Pierini V, Elia L, Mancini M, Propris MS, Apicella V, Gaidano G, Testi AM, Vitale A, Vignetti M, Mecucci C, Guarini A, Cools J, Foà R (2016). RNA sequencing unravels the genetics of refractory/relapsed T-cell acute lymphoblastic leukemia. Prognostic and therapeutic implications. *Haematologica* **101**: 941-950.

Goto Y, Kurozumi A, Arai T, Nohata N, Kojima S, Okato A, Kato M, Yamazaki K, Ishida Y, Naya Y, Ichikawa T, Seki N (2017). Impact of novel miR-145-3p regulatory networks on survival in patients with castration-resistant prostate cancer. *Genetics & Genomics* **117**: 409-420.

Habiel DM, Krepostman N, Lilly M, Cavassani K, Coelho AL, Shibata T, Elenitoba-Johnson K, Hogaboam CM (2016). Senescent stromal cell-induced divergence and therapeutic resistance in T cell acute lymphoblastic leukemia/lymphoma. *Oncotarget* **7**: 83514-83529.

Kato M, Kurozumi A, Goto Y, Nohata N, Arai T, Okato A, Koshizuka K, Kojima S, Ichikawa T, Seki N (2017). Dual-strand tumor-suppressor microRNA-145 (miR-145-5p and miR-145-3p) are involved in castration-resistant prostate cancer pathogenesis. *Cancer Research* **77**: Abstract 1459.

Kordes U, Krappmann D, Heissmeyer V, Ludwig WD, Scheidereit C (2000). Transcription factor NF-κB is constitutively activated in acute lymphoblastic leukemia cells. *Leukemia* **14**: 399-402.

Kuck LR, Saye S, Loob S, Roth-Eichhorn S, Byrne-Nash R, Rowlen KL (2017). VaxArray assessment of influenza split vaccine potency and stability. *Vaccine* **35**: 1918-1925.

Lewis BP, Burge CB, Bartel DP (2005). Conserved seed pairing, often flanked by adenosines, indicates that thousands of human genes are microRNA targets. *Cell* **120**: 15-20.

Lv J, Liang Y, Tu Y, Chen J, Xie Y (2018). Hypoxic preconditioning reduces propofol-induced neuroapoptosis via regulation of Bcl-2 and Bax and downregulation of activated caspase-3 in the hippocampus of neonatal rats. *Neurological Research* **40**: 767-773.

Lv M, Zhang X, Jia H, Li D, Zhang B, Zhang H, Hong M, Jiang T, Jiang Q, Lu J, Huang X, Huang B (2012). An oncogenic role of miR-142-3p in human T-cell acute lymphoblastic leukemia (T-ALL) by targeting glucocorticoid receptor-α and cAMP/PKA pathways. *Leukemia* **26**: 769-777.

Misono S, Seki N, Mizuno K, Yamada Y, Uchida A, Arai T, Kumamoto T, Sanada H, Suetsugu T, Inoue H (2018). Dual strands of the *mi*R-145 duplex (*mi*R-145-5*p* and *mi*R-145-3*p*) regulate oncogenes in lung adenocarcinoma pathogenesis. *Journal of Human Genetics* **63**: 1015-1028.

Nugues A-L, El Bouazzati H, Hétuin D, Berthon C, Loyens A, Bertrand E, Jouy N, Idziorek T, Quesnel B (2014). RIP3 is downregulated in human myeloid leukemia cells and modulates apoptosis and caspase-mediated p65/RelA cleavage. *Cell Death & Disease* **5**: e1384.

Ogasawara N, Kudo T, Sato M, Kawasaki Y, Yonezawa S, Takahashi S, Miyagi Y, Natori Y, Sugiyama A (2018). Reduction of membrane protein CRIM1 decreases E-cadherin and increases claudin-1 and MMPs, enhancing the migration and invasion of renal carcinoma cells. *Biological and Pharmaceutical Bulletin* **41**: 604-611.

Kumoğlu GO, Döşkaya M, Iz SG (2019). The biomarker features of miR-145-3p determined via meta-analysis validated by qRT-PCR in metastatic cancer cell lines. *Gene* **710**: 341-353.

Pan Y, Ye C, Tian Q, Yan S, Zeng X, Xiao C, Wang L, Wang H (2018). miR-145 suppresses the proliferation, invasion and migration of NSCLC cells by regulating the BAX/BCL-2 ratio and the caspase-3 cascade. *Oncology Letters* **15**: 4337-4343.

Qian L, Zhang W, Lei B, He A, Ye L, Li X, Dong X (2016). MicroRNA-101 regulates T-cell acute lymphoblastic leukemia progression and chemotherapeutic sensitivity by targeting Notch1. *Oncology Reports* **36**: 2511-2516.

Raetz EA, Teachey DT (2016). T-cell acute lymphoblastic leukemia. *Hematology, ASH Education Program* **2016**: 580-588.

Seca H, Almeida GM, Guimarães JE, Vasconcelos MH (2010). miR signatures and the role of miRs in acute myeloid leukaemia. *European Journal of Cancer* **46**: 1520-1527.

Shioya M, Obayashi S, Tabunoki H, Arima K, SaitoY, Ishida T, Satoh J (2010). Aberrant microRNA expression in the brains of neurodegenerative diseases: miR-29a decreased in Alzheimer disease brains targets neurone navigator 3. *Neuropathology and Applied Neurobiology* **36**: 320-330.

Szobi A, Rajtik T, Carnicka S, Ravingerova T, Adameova A (2014). Mitigation of postischemic cardiac contractile dysfunction by CaMKII inhibition: effects on programmed necrotic and apoptotic cell death. *Molecular and Cellular Biochemistry* **388**: 269-276.

Teepen JC, Kremer LCM, Ronckers CM, Van Leeuwen FE, Hauptmann M, Van Dulmen-Den BE, Van Der Pal HJ, Jaspers MW, Tissing WJ; Van Den Heuvel-Eibrink, MM, Loonen JJ, Bresters D, Versluys B, Visser OJ (2017). Long-term risk of subsequent malignant neoplasms after treatment of childhood cancer in the DCOG LATER study cohort: role of chemotherapy. *Journal of Clinical Oncology* **35**: JCO2016716902.

Wang S, Liu Z, Wang L, Zhang X (2009). NF-κB signaling pathway, inflammation and colorectal cancer. *Cellular & Molecular Immunology* **6**: 327-334.

Wen F, Yang Y, Jin D, Sun J, Yu X, Yang Z (2014). MiRNA-145 is involved in the development of resistin-induced insulin resistance in HepG2 cells. *Biochemical and Biophysical*

Research Communications **445**: 517-523.

Xia H, Yamada S, Aoyama M, Sato F, Masaki A, Ge Y, Ri M, Ishida T, Ueda T, Utsunomiya A, Asai K, Inagaki H (2014). Prognostic impact of microRNA-145 down-regulation in adult T-cell leukemia/lymphoma. *Human Pathology* **45**: 1192-1198.

Yendamuri S, Calin GA (2009). The role of microRNA in human leukemia: a review. *Leukemia* **23**: 1257-1263.

Yoshino H, Seki N, Hidaka H, Yamasaki T, Idesako T, Yonezawa T, Enokida T, Nakagawa M (2013). MicroRNA expression signatures in bladder cancer: microRNA-145 function as a tumor suppressor through suppression of MAPK and ERBB signaling pathways. *The Journal of Urology* **189**: e377-e378.

Yu L, Li L, Medeiros LJ, Young KH (2017) NF-κB signaling pathway and its potential as a target for therapy in lymphoid neoplasms. *Blood Reviews* **31**: 77-92.

Zhang YC, Ye H, Zeng Z, Chin YE, Huang YN, Fu GH (2015) The NF-κB p65/miR-23a-27a-24 cluster is a target for leukemia treatment. *Oncotarget* **6**: 33554-33567.

Zhao J, Dong D, Sun L, Zhang G, Sun L (2014). Prognostic significance of the epithelial-to-mesenchymal transition markers e-cadherin, vimentin and twist in bladder cancer. *International Braz J Urol* **40**: 179-189.